

# Phase formation and dielectric properties of $0.90\text{Pb}(\text{Mg}_{1/3}\text{Nb}_{2/3})\text{O}_3$ – $0.10\text{PbTiO}_3$ ceramics prepared by a new sol–gel method

K. Babooram, H. Taylor, Z.-G. Ye\*

Department of Chemistry, Simon Fraser University, 8888 University Drive, Burnaby, BC, Canada V5A 1S6

Received 3 December 2003; received in revised form 9 December 2003; accepted 22 December 2003

Available online 10 May 2004

## Abstract

Ceramics of lead magnesium niobate–lead titanate solid solution,  $0.90\text{Pb}(\text{Mg}_{1/3}\text{Nb}_{2/3})\text{O}_3$ – $0.10\text{PbTiO}_3$  (PMN–PT), have been synthesized by a new room temperature sol–gel route, using polyethylene glycol-200 (PEG) and methanol mixture as solvent. The use of a triol molecule, 1,1,1-tris(hydroxymethyl)ethane (THOME), which is known to serve as a complexing agent used in binding together the metal ions in the precursor solution, has been shown to give good dielectric and ferroelectric properties ( $\epsilon'_{\text{max}} = 33,000$  at  $T_{\text{max}} = 40^\circ\text{C}$  and  $P_r = 18\text{ }\mu\text{C}/\text{cm}^2$  at room temperature) for the stoichiometric PMN–PT ceramics sintered at  $1050^\circ\text{C}$ . A 5 mol% excess of lead in the sol–gel process without THOME led to an improvement in the formation of the perovskite phase but a degradation of the dielectric properties with  $\epsilon'_{\text{max}} = 10,000$  and  $P_r = 11\text{ }\mu\text{C}/\text{cm}^2$  only.

© 2004 Elsevier Ltd and Techna Group S.r.l. All rights reserved.

**Keywords:** A. Sol–gel process; C. Electrical properties; C. Ferroelectric properties; D. Perovskites; E. Capacitors; Ceramics

## 1. Introduction

The relaxor ferroelectric solid solution system,  $(1-x)\text{Pb}(\text{Mg}_{1/3}\text{Nb}_{2/3})\text{O}_3$ – $x\text{PbTiO}_3$  [ $(1-x)\text{PMN}$ – $x\text{PT}$ ], has attracted considerable interest because of its remarkable dielectric and electromechanical properties in the form of ceramics and single crystals [1–3].  $\text{Pb}(\text{Mg}_{1/3}\text{Nb}_{2/3})\text{O}_3$  (PMN) is well-known to exhibit typical relaxor ferroelectric behavior characterized by a broad and frequency dependent dielectric maximum at  $T_{\text{max}}$  (around  $-15^\circ\text{C}$ ) [4]. Addition of the normal ferroelectric  $\text{PbTiO}_3$  (PT) to PMN shifts this transition temperature upwards, enhances the dielectric properties of the solid solutions, and induces a long-range ferroelectric phase [5,6]. A morphotropic phase boundary (MPB) appears in the region of 30–37 mol% PT with the presence of a rhombohedral, a tetragonal, and a newly discovered monoclinic phase [5,7]. As a result, the  $(1-x)\text{PMN}$ – $x\text{PT}$  system embraces a wide range of compositions which find important applications in multi-layer

dielectric capacitors, piezoelectric devices, and sensors and actuators [8]. The PMN–PT system exhibits excellent piezo-/ferroelectric properties but also a higher stability of the perovskite structure compared to other relaxor-based systems such as  $(1-x)\text{Pb}(\text{Zn}_{1/3}\text{Nb}_{2/3})\text{O}_3$ – $x\text{PbTiO}_3$  (PZNT) and  $(1-x)\text{Pb}(\text{Sc}_{1/2}\text{Nb}_{1/2})\text{O}_3$ – $x\text{PbTiO}_3$  (PSNT) [3]. Being close to the PMN side of the  $(1-x)\text{PMN}$ – $x\text{PT}$  phase diagram,  $0.90\text{PMN}$ – $0.10\text{PT}$  is a typical relaxor ferroelectric material with a weak rhombohedral distortion [6]. It exhibits high dielectric permittivity, narrow hysteresis loop, and strong piezoelectric response, which together make it an excellent material for multi-layered high density capacitors [8].  $0.90\text{PMN}$ – $0.10\text{PT}$  has a diffuse phase transition temperature ( $T_{\text{max}}$ ) at about  $40^\circ\text{C}$  and its dielectric constant at room temperature is very high ( $\epsilon' \sim 10,000$ ), making it a potential candidate for DRAM and multi-layer capacitor applications [9].

The synthesis of pure perovskite  $0.90\text{PMN}$ – $0.10\text{PT}$  by conventional solid state reactions can be very challenging due to the formation of a thermodynamically more stable but undesired impurity phase of pyrochlore structure which considerably impairs the dielectric properties of the material [10]. As a result, a number of different soft

\* Corresponding author. Tel.: +1-604-291-3351;  
fax: +1-604-291-3765.

E-mail address: zye@sfu.ca (Z.-G. Ye).

chemistry techniques like sol–gel and solution processes have been designed for the synthesis of pure perovskite 0.90PMN–0.10PT [11–13]. The polymeric precursor method, which is based on the Pechini's technique, has become very popular in the making of fine mixed-metal oxide powders [14–16]. This solution process consists of preparing a polymer–cation complex in solution and then converting it into the multi-component oxide by burning out the organic components during high-temperature treatment [17]. The main feature of this method is that it allows a very homogeneous dispersion of the cations in the polymer–cation complexes, which helps in the formation of fine and highly reactive mixed oxide powders [18].

Polyethylene glycol (PEG) has proved to be a very suitable polymer for use in the polymeric precursor method in the preparation of mixed oxide powder and ceramics. The reason for this is the coordination of the ether oxygen atoms in PEG to the metal cations, which allows it to dissolve a number of inorganic salts as well as metal alkoxides. Besides the polymer-binding, cross-linking can also greatly help in obtaining a very homogeneous distribution of cations in solutions. Sriprang et al. used a triol, 1,1,1-tris(hydroxymethyl)ethane (THOME) as a cross-linking agent for the cations in the synthesis of lead zirconate titanate thin films [19]. They demonstrated that with its three hydroxyl groups, THOME could bind to up to three metal ions at a time, forming oligomeric species that were then oxidized to form the final mixed oxide compound.

In our recent work, we have prepared 0.65PMN–0.35PT ceramics using a room temperature soft chemistry route [20] using a mixture of PEG200 and methanol as solvent and THOME as a complexing agent. Pure perovskite phase, high density, high dielectric constant, and excellent ferroelectric properties were obtained for the ceramics prepared from a stoichiometric amount of the lead starting material in the preparation of the sol. A decrease in the ceramic quality in terms of the perovskite phase purity and dielectric properties was observed in those ceramics prepared without using THOME in the reaction. In this work, we successfully apply this new room temperature soft chemistry route based on polyethylene glycol to the synthesis of 0.90PMN–0.10PT ceramics and characterized their dielectric and ferroelectric properties in relation to the preparation conditions.

## 2. Experimental procedure

The 0.90PMN–0.10PT ceramics have been prepared by a new soft chemistry route. The starting materials used were lead(II) acetate trihydrate ( $\text{Pb}(\text{CH}_3\text{COO})_2 \cdot 3\text{H}_2\text{O}$ ), magnesium 2,4-pentanedionate dihydrate ( $\text{Mg}(\text{O}_2\text{C}_5\text{H}_7)_2 \cdot 2\text{H}_2\text{O}$ ), niobium(V) ethoxide ( $\text{Nb}(\text{OC}_2\text{H}_5)_5$ ), titanium diisopropoxidebis(acetylacetonate) ( $\text{Ti}(\text{OC}_3\text{H}_7)_2(\text{O}_2\text{C}_5\text{H}_7)_2$ ) (TIAA). Stoichiometric amounts of  $\text{Pb}(\text{CH}_3\text{COO})_2 \cdot 3\text{H}_2\text{O}$ ,  $\text{Mg}(\text{O}_2\text{C}_5\text{H}_7)_2 \cdot 2\text{H}_2\text{O}$ , and 1,1,1-tris(hydroxymethyl)ethane ( $\text{C}(\text{CH}_2\text{OH})_3(\text{CH}_3)$ ) were dissolved in a 1:2 volume mixture

of polyethylene glycol 200 (PEG) and methanol (MeOH) by simple stirring at room temperature to give a clear, yellow solution. In a separate flask,  $\text{Nb}(\text{OC}_2\text{H}_5)_5$ , TIAA, and THOME were mixed and stirred in the PEG/MeOH mixture under the same conditions to yield a light orange clear solution. These two solutions were then mixed together and further stirred at room temperature for about 6 h, at the end of which a clear yellow solution was formed. The volatile organic species were evaporated by means of rotary evaporator, giving rise to a very viscous precursor sol, which was then burnt at 500 °C for 2 h to form a light orange powder. The powder was ground in acetone, pressed into discs and calcined at various temperatures between 650 and 1050 °C for 8 h. These as-prepared 0.90PMN–0.10PT ceramics were abbreviated as 10PEG(S)T. The same procedure was employed to prepare three other 0.90PMN–0.10PT ceramics under various conditions: (i) stoichiometric amount of lead(II) acetate and no THOME (named 10PEG(S)), (ii) 5 mol% excess of lead(II) acetate with THOME (named 10PEG(5)T), and (iii) 5 mol% excess of lead(II) acetate and no THOME (named 10PEG(5)), in order to study the effects of the chemical parameters on the quality and properties of the resulting ceramics.

The phases of the samples were checked by X-ray powder diffraction using Cu K $\alpha$  radiation (46 kV, 42 mA) on a Rigaku X-ray diffractometer. The decomposition process of the precursor solutions was investigated by thermogravimetric (TG) and differential thermal analyses (DTA) on a Seiko Exstar 6300 TG/DTA Thermal Analyzer. The precursor sols were oxidized by heating from room temperature to 1000 °C in air at a heating rate of 5 °C/min. The temperature and frequency dependence of the dielectric permittivity of the ceramics were measured on an Alpha High Resolution Dielectric/Impedance Analyzer (Novocontrol). Ferroelectric hysteresis loops were displayed on a RT66A Standard Ferroelectric Testing System by applying a field of  $E = \pm 23$  kV/cm across the ceramics.

## 3. Results and discussion

### 3.1. Thermogravimetry/differential thermal analysis (TG/DTA)

The best conditions for the pyrolysis of the precursor solutions and for the sintering of the precursor powders were determined by thermal analyses. Fig. 1a and b show the DTA/TG curves of the 10PEG(S)T and 10PEG(5) precursor solutions, respectively, from room temperature to 1000 °C at a heating rate of 5 °C/min. Three different weight loss regions can be observed on the TGA curve of the 10PEG(S)T precursor solution. The first one in the region of 45–120 °C indicates the volatilization of solvent and/or moisture still present in the precursor solution. A second weight loss appears in the region of 120–325 °C, which can be attributed to the decomposition of the PEG chains,

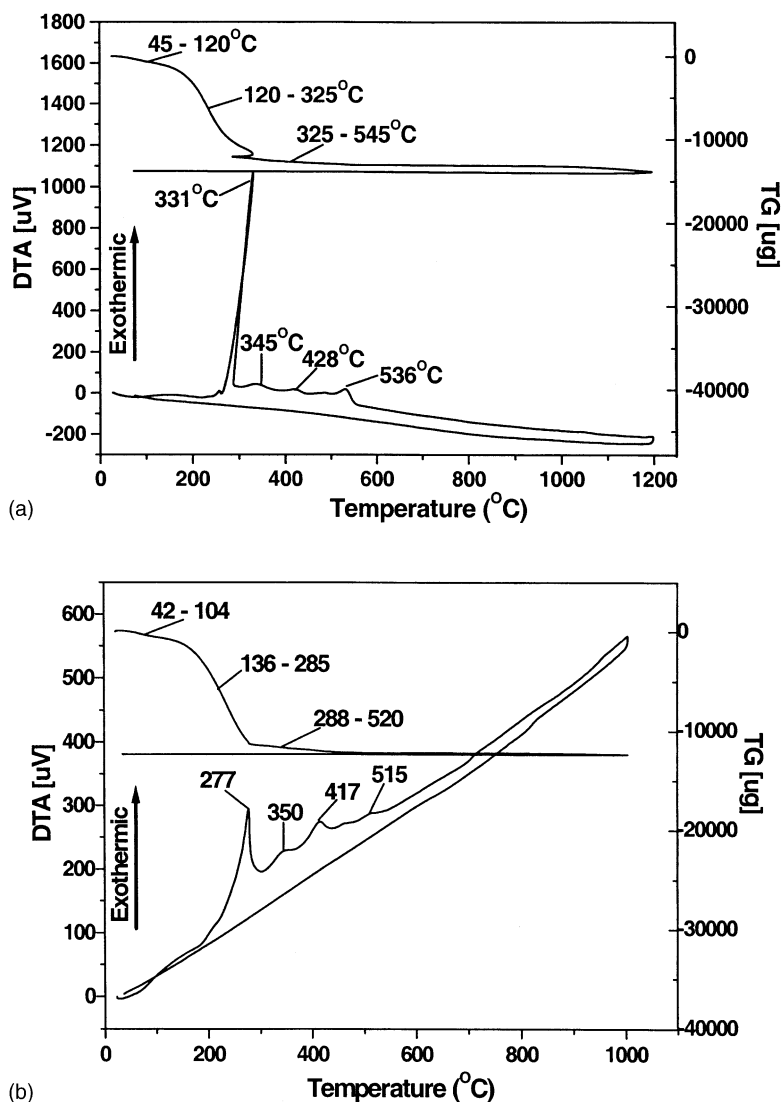


Fig. 1. TG/DTA curves from room temperature to 1000 °C at a heating rate of 5 °C/min for (a) 10PEG(S)T and (b) 10PEG(5) precursor solutions.

the THOME molecules, and the acetate groups present in the sol. The third weight loss occurring between 325 and 545 °C is assigned to the decomposition of the complex structures in the sol, which can be the PEG chains and/or the THOME molecules bound to the metal centres. This process was accompanied by a strong exothermic peak at 331 °C on the DTA curve. The other exothermic peaks at 345 and 428 °C are the result of the decomposition of more complex metal–organic structures or oligomers that were formed from condensation reactions in the precursor solution. The small exothermic peak at 536 °C can be attributed to the formation of the crystalline mixed oxide phase. These observations lead to the conclusion that all the organic moieties present in the precursor solution are oxidized and decomposed at temperatures below ~450 °C, after which the resulting matter undergoes a rearrangement of the M–O–M networks to form the crystalline pyrochlore phase at around 536 °C.

The 10PEG(5) precursor solution exhibits similar thermal behaviour. The differences here lie in the absence of

the THOME molecule and the presence of a 5 mol% excess of lead in the sol–gel process. Three weight loss regions are also observed on the TG curve shown in Fig. 1b, which are at 42–104, 136–285, and 288–520 °C, corresponding to (i) the volatilization of the solvent and/or moisture present in the precursor solution, (ii) the decomposition of the PEG–cation complexes, and (iii) the decomposition of more complex PEG–metal structures or oligomers, respectively. The exothermic peaks observed on the DTA curve (Fig. 1b) at 277, 350, and 417 °C result from the thermal processes associated with the second and third weight losses, respectively. The exothermic peak at 515 °C is assigned to the crystallization of the oxide phases that are a mixture of the perovskite and pyrochlore phases, as revealed by X-ray diffraction (see Section 3.2). The first exothermic peak occurs at a temperature (277 °C) lower than that in the 10PEG(S)T sol (331 °C). This strongly supports the fact that both the PEG chains and the THOME molecules chelate to the metal centres in the 10PEG(S)T sol, forming more

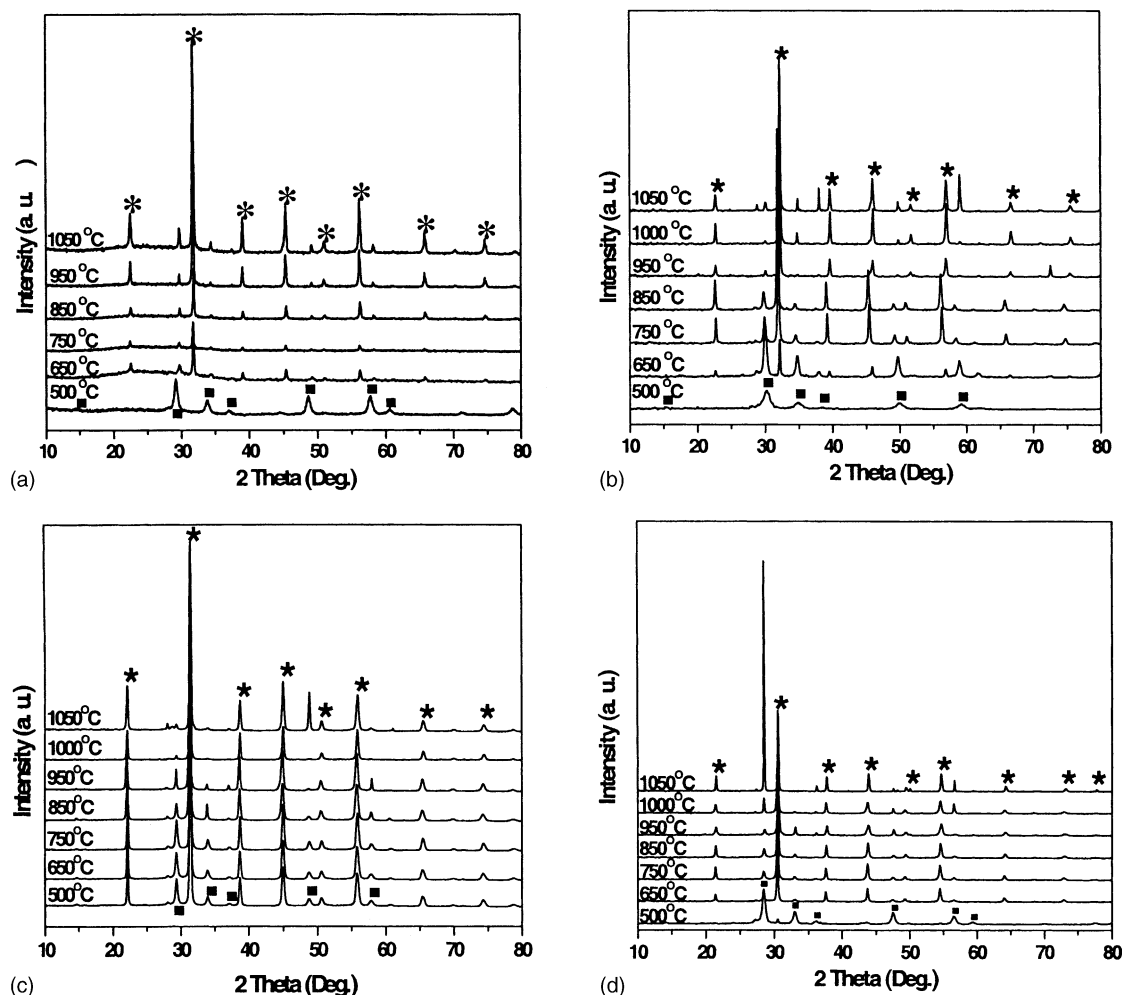


Fig. 2. X-ray diffraction spectra at different calcination temperatures of (a) 10PEG(S)T, (b) 10PEG(S), (c) 10PEG(5), and (d) 10PEG(5)T precursor powders. All samples were calcined for a period of 8 h. (■): Pyrochlore phase; (★): Perovskite phase.

complex structures that decompose at a higher temperature. In the 10PEG(5) sol, however, only the PEG chains can bind to the cations through their hydroxyl end groups and the ether oxygens present in the polymer backbone.

### 3.2. Phase analysis by X-ray diffraction

Powder X-ray diffraction (XRD) was used to check the phases in all the samples. The XRD patterns of the 10PEG(S)T, 10PEG(S), 10PEG(5), and 10PEG(5)T samples synthesized at different temperatures are shown in Fig. 2a–d, respectively. It can be seen that crystallization already occurred at 500 °C in all the samples, with the formation of the pyrochlore phase in the 10PEG(S)T and 10PEG(S) samples, and a mixture of the perovskite and the pyrochlore phases in the 10PEG(5) and 10PEG(5)T samples. Upon heating, the perovskite phase grows at the expense of the pyrochlore phase in all cases. In the 10PEG(5) sample, an almost pure perovskite phase appears at 1000 °C, above which, the impure phase seems to grow slightly upon further heating. In the case of 10PEG(S)T and

10PEG(S), the perovskite phase appears as the major phase after thermal treatment at 950 and 1000 °C, respectively, but a small amount (<10%) of pyrochlore phase persists.

Fig. 3a and b show the plots of the amount of perovskite phase formed as a function of the sintering temperature for the 10PEG(S)T and 10PEG(S), and the 10PEG(5) and 10PEG(5)T ceramics, respectively. For 10PEG(S)T (Fig. 3a), as the sintering temperature is increased, the amount of perovskite phase also increases from 75% at 650 °C to a maximum of 91% at 950 °C, after which it drops down to ~88% at 1050 °C. In the case of 10PEG(S), the amount of perovskite phase formed after treatment at 650 °C is about 42%. It increases to a maximum of ~91% at 1000 °C (Fig. 3a). For 10PEG(5) (Fig. 3b), the sample treated at 500 °C already contains more than 87% of perovskite phase. Upon further heating, the amount of the perovskite phase increases to a maximum of ~96% at 1000 °C and then decreases to ~93% at 1050 °C. The 10PEG(5)T sample treated at 500 °C contains ~20% of the perovskite phase, which increases to a maximum of about 85% at 750 °C, after which it drops considerably down to

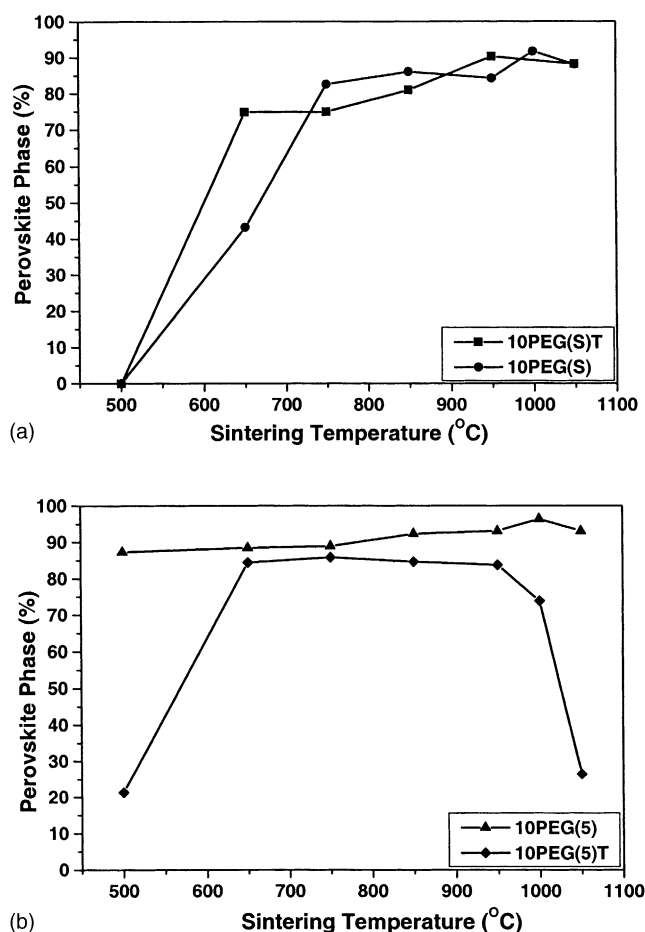


Fig. 3. Dependence of the amount of the perovskite phase formation on the sintering temperature of the (a) 10PEG(S)T and 10PEG(S), and (b) 10PEG(5) and 10PEG(5)T ceramics.

only  $\sim 25\%$  at  $1050^\circ\text{C}$  (Fig. 3b). These results indicate that (i) the 10PEG(S)T and 10PEG(S) ceramics exhibit similar behaviour in terms of the formation of the perovskite phase with a maximum percentage of about 91%, (ii) a 5 mol% excess of lead in the precursor powder favors the formation of the perovskite phase at a temperature as low as  $500^\circ\text{C}$  in both 10PEG(5) and 10PEG(5)T, but the former contains considerably more perovskite phase in a larger temperature range, (iii) the presence of a 5% excess of lead in the precursor solution improves the maximal amount of the perovskite phase formed by 2–5% in the 10PEG(5) ceramics as compared to the 10PEG(S)T ceramics sintered at the same temperature, (iv) the 5% excess of lead without THOME results in the highest percentage of the perovskite phase (96%), while the combination of an excess of lead and THOME in the precursor solution leads to a maximum perovskite phase of about 85% only with a much narrower temperature stability range as compared to 10PEG(5).

### 3.3. Dielectric measurements

Fig. 4a and b illustrate the temperature and frequency dependences of the real part of the dielectric permittivity ( $\epsilon'$ )

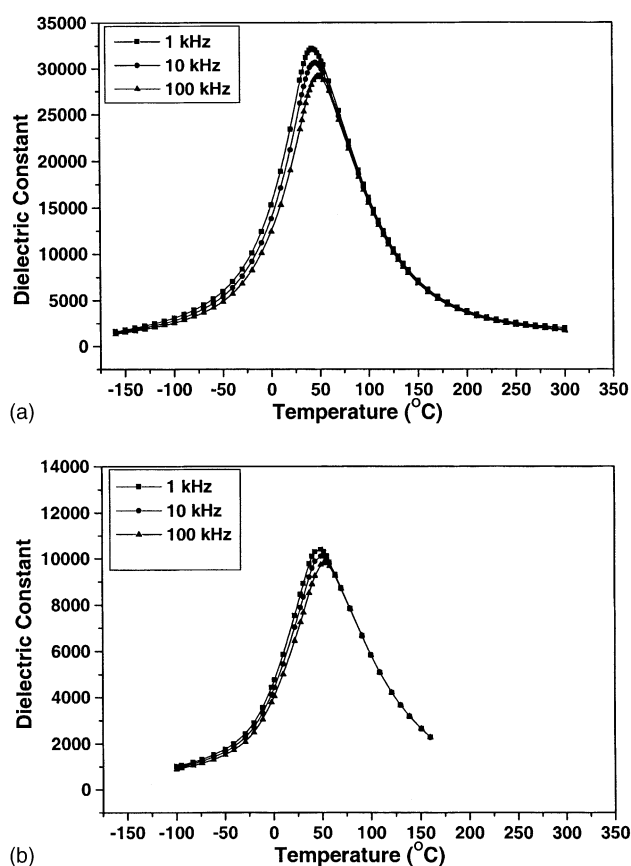


Fig. 4. Variation of the dielectric constant as a function of temperature at different frequencies for (a) 10PEG(S)T and (b) 10PEG(5) ceramics sintered at  $1050^\circ\text{C}$  and  $1000^\circ\text{C}$  for 8 h, respectively.

of the 10PEG(S)T and 10PEG(5) ceramics sintered at  $1050^\circ\text{C}$  and  $1000^\circ\text{C}$ , respectively, with a relative density of 95%. As can be observed from these curves, the dielectric constant shows a diffuse and frequency-dependent maximum with the temperature of the maximal permittivity ( $T_{\text{max}} \approx 40^\circ\text{C}$ ) increasing, while the value of the permittivity maximum ( $\epsilon'_{\text{max}}$ ) decreases, as the frequency increases. This indicates a typical relaxor ferroelectric behaviour for the both ceramics of 0.90PMN–0.10PT. The 10PEG(S)T ceramic shows a room temperature dielectric constant of nearly 25,000 and a maximum value of  $\epsilon'_{\text{max}} = 33,000$  at  $T_{\text{max}} \approx 40^\circ\text{C}$  (1 kHz). It is worth noting that these dielectric constant values are considerably higher than those obtained by solid state reactions [10] or by other sol–gel processes [11]. On the other hand, the 10PEG(5) ceramic shows a much lower dielectric constant value of  $\sim 8000$  at room temperature and an  $\epsilon'_{\text{max}}$  of  $\sim 10,000$  at  $T_{\text{max}}$ . The dielectric measurements of the 10PEG(S) sample sintered at  $1000^\circ\text{C}$  gave rise to a room temperature dielectric constant of 12,500 and an  $\epsilon'_{\text{max}}$  of  $\sim 19,700$  at  $T_{\text{max}} \sim 42^\circ\text{C}$  (not shown).

The high value of the dielectric constant in the 10PEG(S)T ceramic can be attributed to the presence of the THOME molecule in the sol–gel process. Its beneficial role in the sol–gel preparation of 0.65PMN–0.35PT ceramics using

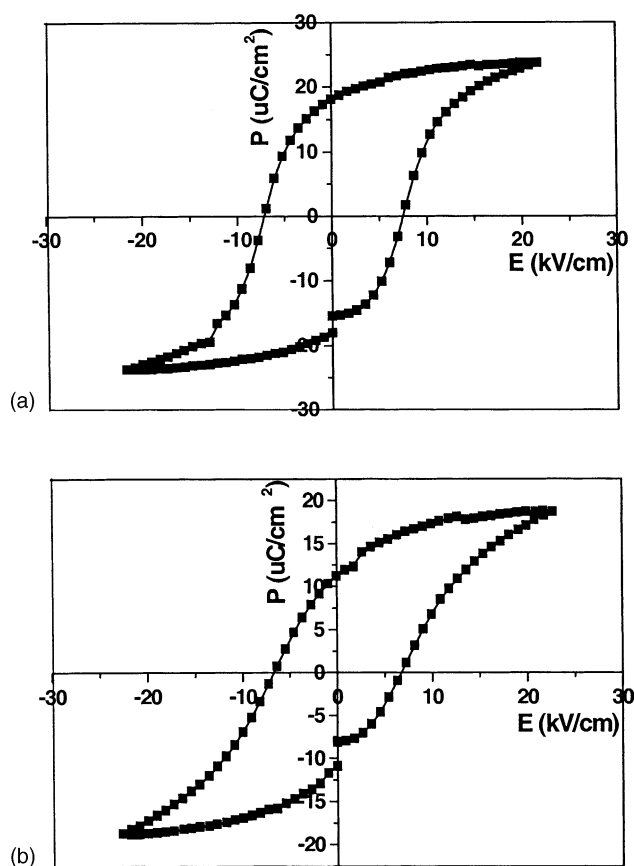


Fig. 5. Variation of polarization as a function of bipolar electric field for (a) 10PEG(S)T and (b) 10PEG(5) ceramics sintered at 1050 and 1000 °C, respectively, for 8 h showing ferroelectric hysteresis loops.

polyethylene glycol-200 and methanol as solvent has been highlighted in our recent work [20]. The presence of three hydroxyl groups on the THOME molecule allows it to complex to the metal centres, leading to formation of cross-linked or oligomeric species in solution [19]. This favors the formation of the M–O–M bonds and their easy arrangement into a more homogeneous local structure after the organic components are burnt off, leading to a dense ceramic with excellent dielectric properties after sintering at a relatively low temperature of 950 °C. Although an excess of lead can improve the formation of the perovskite phase to some extent, it can more drastically degrade the dielectric properties of the resulting ceramic, especially in combina-

tion with THOME. This is shown by the considerable lowering of the room temperature dielectric constant and  $\epsilon'_{\max}$  in 10PEG(5), as compared to 10PEG(S)T. The dielectric properties of the stoichiometric 10PEG(S) without THOME are intermediate between 10PEG(S)T and 10PEG(5).

### 3.4. Ferroelectric measurements

The ferroelectric hysteresis loops of the 10PEG(S)T and 10PEG(5) ceramics sintered at 1050 and 1000 °C are shown in Fig. 5a and b, respectively. Both ceramics have a coercive field,  $E_c$ , of about 7.5 kV/cm. The 10PEG(S)T ceramic shows a well-defined and saturated ferroelectric hysteresis loop with a remnant polarization ( $P_r$ ) of 18  $\mu\text{C}/\text{cm}^2$  which is higher than that of 10PEG(5) ( $P_r = 11 \mu\text{C}/\text{cm}^2$ ). The improved ferroelectric properties of the 10PEG(S)T ceramic can also be attributed to the presence of the THOME molecule in the sol–gel synthesis, leading to a dense morphology and good dielectric performance. These properties make the material promising for applications in advanced electromechanical devices. The presence of excess lead in the 10PEG(5) ceramic is again detrimental to the ferroelectricity as it lowers the  $P_r$  of the compound. The 10PEG(S) ceramic sample sintered at 1000 °C shows a coercive field of  $\sim 7.5$  kV/cm and a remnant polarization of 19  $\mu\text{C}/\text{cm}^2$  (not shown), which are very close to the results obtained in 10PEG(S)T.

## 4. Conclusions

Relaxor ferroelectric 90% PMN–10% PT ceramics have been synthesized by a new room temperature soft chemistry route which uses polyethylene glycol-200 and methanol as solvent. The effects of the various chemical processes in the sol–gel preparation on the phase formation and the dielectric and ferroelectric properties of the 0.90PMN–0.10PT ceramics have been systematically investigated. The results are summarized in Table 1.

It is found that the use of a complexing agent, 1,1,1-tris(hydroxymethyl)ethane, and a stoichiometric amount of the lead starting chemical leads to the 10PEG(S)T ceramic of best overall results, with excellent dielectric and ferroelectric properties ( $\epsilon'(\text{PT}) = 25,000$ ,  $\epsilon'_{\max} = 33,000$ , and  $P_r = 18 \mu\text{C}/\text{cm}^2$ ) and a perovskite phase of over

Table 1

Phase formation and properties of 90% PMN–10% PT ceramics prepared under various conditions

	Phase		Properties				
	Perovskite (maximum %)	Sintering temperature	$\epsilon'(\text{RT})^a$	$\epsilon'_{\max}^a$	$T_{\max}^a$ (°C)	$P_r(\text{RT})$ ( $\mu\text{C}/\text{cm}^2$ )	Rank <sup>b</sup>
10PEG(S)T	90.3	950	25000	33000	40	18	1
10PEG(S)	91.7	1000	12500	19700	42	19	2
10PEG(5)	96.4	1000	8000	10000	40	11	3
10PEG(5)T	85.9	750	–	–	–	–	4

<sup>a</sup> At 1 kHz.

<sup>b</sup> 1, best; 4, worst.

90% purity. These dielectric properties are not only significantly better than the results reported previously on the 0.90PMN–0.10PT ceramics, but also better than the 10PEG(S) ceramic prepared without THOME that contains about the same amount of the perovskite phase. This suggests that the use of the THOME (triol) molecule has enhanced the dielectric properties of the 0.90PMN–0.10PT ceramics. Based on the thermal analyses, it is believed that the THOME molecule actively takes part in the sol–gel process by binding to the metal centre to form cross-linked or oligomeric species, which favors the formation of the M–O–M bonds and their easy arrangement into a more homogeneous local structure after sintering at a relatively low temperature of 950 °C. The introduction of a 5 mol% excess of lead in the sol–gel process without THOME has improved the formation of the perovskite phase by 2–5%, but it has more drastically degraded the dielectric properties of the 10PEG(5) ceramic. Interestingly, the combination of an excess of lead and the use of THOME has led to the worst results in the 10PEG(5)T ceramic both in terms of the perovskite phase formation and the properties.

## Acknowledgements

This work was supported by the Natural Science and Engineering Research Council of Canada (NSERC).

## References

- [1] S.J. Jang, K. Uchino, S. Nomura, L.E. Cross, Electrostrictive behavior of lead magnesium niobate based ceramic dielectrics, *Ferroelectrics* 27 (1980) 31–34.
- [2] S.-E. Park, T.R. Shrout, Ultrahigh strain and piezoelectric behavior in relaxor based ferroelectric single crystals, *J. Appl. Phys.* 82 (4) (1997) 1804–1811.
- [3] Z.-G. Ye, M. Dong, Morphotropic domain structures and phase transitions in relaxor-based piezo-/ferroelectric  $(1-x)\text{Pb}(\text{Mg}_{1/3}\text{Nb}_{2/3})\text{O}_3-x\text{PbTiO}_3$  single crystals, *J. Appl. Phys.* 87 (5) (2000) 2312–2319.
- [4] Z.-G. Ye, Relaxor ferroelectric complex perovskites: structure, properties and phase transitions, *Key Eng. Mater.* 155–156 (1998) 81–122.
- [5] T.R. Shrout, Z.P. Chang, N. Kim, S. Markgraf, Dielectric behavior of single crystals near the  $(1-x)\text{Pb}(\text{Mg}_{1/3}\text{Nb}_{2/3})\text{O}_3-x\text{PbTiO}_3$  morphotropic phase boundary, *Ferroelectr. Lett.* 12 (1990) 63–69.
- [6] Z.-G. Ye, Y. Bing, J. Gao, A.A. Bokov, Development of ferroelectric order in relaxor  $(1-x)\text{Pb}(\text{Mg}_{1/3}\text{Nb}_{2/3})\text{O}_3-x\text{PbTiO}_3$  ( $0 \leq x \leq 0.15$ ), *Phys. Rev. B* 67 (2003) 104104-1-8.
- [7] B. Noheda, D.F. Cox, G. Shirane, J. Gao, Z.-G. Ye, Phase diagram of the ferroelectric relaxor  $(1-x)\text{PbMg}_{1/3}\text{Nb}_{2/3}\text{O}_3-x\text{PbTiO}_3$ , *Phys. Rev. B* 66 (2002) 054104.
- [8] R.F. Newnham, Q.C. Xu, S. Kumar, L.E. Cross, Smart ceramics, *Ferroelectrics* 102 (1990) 259.
- [9] L.F. Francis, D.A. Payne, Thin-layer dielectrics in the  $\text{Pb}[(\text{Mg}_{1/3}\text{Nb}_{2/3})_{1-x}\text{Ti}_x]\text{O}_3$  system, *J. Am. Ceram. Soc.* 74 (12) (1991) 3000–3010.
- [10] S.L. Swartz, T.R. Shrout, W.A. Schulze, L.E. Cross, Dielectric properties of lead magnesium niobate ceramics, *J. Am. Ceram. Soc.* 67 (5) (1984) 311–315.
- [11] P. Ravindranathan, S. Komareni, A.S. Bhalla, R. Roy, Synthesis and dielectric properties of sol–gel-derived 0.9Pb( $\text{Mg}_{1/3}\text{Nb}_{2/3}$ ) $\text{O}_3$ –0.1PbTiO<sub>3</sub> ceramics, *J. Am. Ceram. Soc.* 74 (12) (1991) 2996–2999.
- [12] F. Chaput, J.P. Boilot, M. Lejeune, R. Papiernik, L.G. Hubert Pfalzgraf, Low-temperature route to lead magnesium niobate, *J. Am. Ceram. Soc.* 72 (8) (1989) 1355–1357.
- [13] Y. Narendar, G.L. Messing, Kinetic analysis of combustion synthesis of lead magnesium niobate from metal carboxylate gels, *J. Am. Ceram. Soc.* 80 (4) (1997) 915–924.
- [14] M.P. Pechini, Method of preparing lead and alkaline earth titanates and niobates and coating method using the same to form a capacitor, US Patent No. 3 330 697 (1967).
- [15] P.A. Lessing, Mixed-cation oxide powders via polymeric precursors, *Am. Ceram. Soc. Bull.* 68 (1989) 1002–1007.
- [16] L.-W. Tai, P.A. Lessing, Modified resin-intermediate processing of perovskite powders. Part I. Optimization of polymeric precursors. Part II. Processing for fine, nonagglomerated Sr-doped lanthanum chromite powders, *J. Mater. Res.* 7 (1992) 502–519.
- [17] S.C. Zhang, G.L. Messing, W. Huebner, M.M. Coleman, Synthesis of  $\text{YBa}_2\text{Cu}_3\text{O}_{7-x}$  fibers from an organic acid solution, *J. Mater. Res.* 5 (1990) 1806–1812.
- [18] N. Uekawa, M. Endo, K. Kakegawa, Y. Sasaki, Homogeneous precipitation of  $\text{Cr}^{3+}$ – $\text{M}^{2+}$  ( $\text{M} = \text{Ni}, \text{Zn}, \text{Co}, \text{Cu}$ ) oxalate by oxidation of the polyethylene glycol–cation complex, *Phys. Chem. Chem. Phys.* 2 (2000) 5485–5490.
- [19] N. Sriprang, D. Kaewchinda, J.D. Kennedy, S.J. Milne, Processing and sol chemistry of a triol-based sol–gel route for preparing lead zirconate titanate thin films, *J. Am. Ceram. Soc.* 83 (8) (2000) 1914–1920.
- [20] K. Babooram, Z.-G. Ye, Polyethylene glycol-based new solution route to relaxor ferroelectric  $0.65\text{Pb}(\text{Mg}_{1/3}\text{Nb}_{2/3})\text{O}_3$ – $0.35\text{PbTiO}_3$ , unpublished.